Results in Engineering 25 (2025) 104022

Contents lists available at ScienceDirect

Results in Engineering

journal homepage: www.sciencedirect.com/journal/results-in-engineering

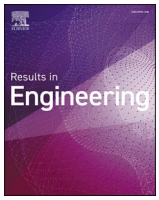

Evaluating the impact of roof rainwater harvesting on hydrological connectivity and urban flood mitigation

Quang-Oai Lu [a,b], Reza Bahramloo [c], Jesús Rodrigo-Comino [d], Jun Wang [e], Ali Talebi [f], Quynh Thi Phuong Tran [g,*], Afshin Ghahramani [h], Mehdi Sepehri [i]

[a] Advanced Applied Sciences Research Group, Dong Nai Technology University, Bien Hoa City, Vietnam
[b] Faculty of Technology, Dong Nai Technology University, Bien Hoa City, Vietnam
[c] Agricultural Engineering Research Department, Hamedan Agricultural and Natural Resources Research and Education Center, AREEO, Hamedan, Iran
[d] Departamento de Análisis Geográfico Regional y Geografía Física, Facultad de Filosofía y Letras, Campus Universitario de Cartuja, Universidad de Granada, 18071, Granada, Spain
[e] School of Civil Engineering, Shandong University, Jinan, Shandong Province, 250061, PR China
[f] Department of Watershed Management, Faculty of Natural Resources, Yazd University, Yazd, Iran
[g] Faculty of Environment and Labour Safety, Ton Duc Thang University, Ho Chi Minh City, Vietnam
[h] Department of Environment, Tourism, Science and Innovation, Queensland Government, Toowoomba, QLD 4350, Australia
[i] Rangeland Department, Research Institute of Forests and Rangelands, Tehran, Iran

ARTICLE INFO

Keywords:
Roof rainwater harvesting
Urban flooding
Hydrological connectivity
Catchment

ABSTRACT

Urban flooding, particularly in arid and semi-arid regions, has become a growing concern in densely populated metropolitan areas. Roof rainwater harvesting is a form of low impact development that offers an effective solution for mitigating urban flooding, particularly in densely populated metropolitan areas. However, few scientific studies have attempted to model this dynamic, allowing us to increase water collection and reduce the risk of floods, especially in arid and semiarid areas. This study examined the impact of Roof rainwater harvesting on flood severity using the Borselli index of connectivity, which quantifies the degree to runoff connectivity between upstream and downstream areas, reflecting the potential for runoff to contribute to flooding. As a case study, we selected Hamadan, one of the world's oldest cities. The methodology involved quantifying HC under two scenarios: with and without Roof rainwater harvesting implementation. The results demonstrated a substantial reduction in hydrological connectivity when Roof rainwater harvesting was implemented, highlighting the valuable effectiveness of Roof rainwater harvesting. In contrast, without Roof rainwater harvesting, most of the areas, particularly in the middle and northern regions, had a high degree of hydrological connectivity. Overall, with the incorporation of RRWH, there was a significant shift toward increased connectivity. The areas characterized by very high and high degrees of hydrological connectivity in the absence of Roof rainwater harvesting decreased to 11.4 % and 20.4 %, respectively. Conversely, the moderate, low, and very low hydrological connectivity categories experienced increases of 27.9, 28.4, and 11.7 %, respectively. We conclude that this new evaluation of hydrological connectivity can serve as a valuable tool for assessing hydrological connectivity in urban areas and reveal to land managers where Roof rainwater harvesting is not effectively applied and where possible improvements must be made. However, the success of Roof rainwater harvesting in urban areas depends on technical, social, and regulatory support, as well as public acceptance for non-potable uses.

1. Introduction

Floods are known as common natural hazards after extreme precipitation events are concentrated, usually occurring over short periods; however, floods can occur due to interfering anthropogenic factors such as poor or erroneous land use planning, rapid population

Abbreviations: RRWH, Roof rainwater harvesting; LID, Low impact development; HC, Hydrological connectivity; RWH, Rainwater harvesting; MCDA, Multi Criteria Decision Making; SCS-CN, Soil Conservation Service Curve Number; RUSLE, The Revised Universal Soil Loss Equation; AMC, Antecedent moisture condition; DEM, Digital elevation model; FCFs, Fine constrained features; CD-TIN, Constrained Delaunay triangle irregular network.

* Corresponding author.
E-mail address: tranthiphuongquynh@tdtu.edu.vn (Q.T.P. Tran).

https://doi.org/10.1016/j.rineng.2025.104022
Received 18 November 2024; Received in revised form 3 January 2025; Accepted 12 January 2025
Available online 16 January 2025
2590-1230/© 2025 The Authors. Published by Elsevier B.V. This is an open access article under the CC BY-NC-ND license (http://creativecommons.org/licenses/by-nc-nd/4.0/).

growth and low socioeconomic control measures [1–4]. Hazard terms will be transferred to disasters when dramatic consequences such as loss of life, injury or other health impacts, property damage, social and economic disruption or environmental degradation occur [5–7]. Currently, the world is experiencing noncontrolled urbanization and land use changes, which have far-reaching consequences [8–11].

Urbanization is accompanied by the escalation of imperviousness, causing uncontrolled and unknown hydrological responses even at the regional scale; thus, the majority of storms that occur progress to extreme runoff rates even for those with low return periods [12–15]. By increasing the return period, runoff occurrence could inevitably cause more frequent destructive floods to threaten built and infrastructure [16–19]. Globally, from 1985 to 2020, the area of impervious surfaces doubled from 5.116×10^5 to 10.871×10^5 km^2, and Asian countries with a total increase in 2.946×10^5 km^2 experienced greater growth than did other countries [20–22].

The escalating phenomenon of climate change, exacerbated by human activities, is linked with urban sprawl, forming an intricate union that poses unknown consequences for hydrological processes [3,23–25]; W. [26]. The amplification of these human activities (industries, urbanization, intensification of agriculture and rangelands, etc.) is intensifying the greenhouse effect, leading to global warming and altering precipitation patterns [27,28]. Urban sprawl further compounds these challenges by altering land cover and increasing impervious surfaces and soil sealing, disrupting natural hydrological cycles [29–31]. Impervious surfaces hinder infiltration, augment surface runoff, and alter the timing and magnitude of peak flows in watersheds. This phenomenon can modify the equilibrium of ecosystems and exacerbate the frequency and intensity of flooding events [29,32–34]. Urbanization influences the temperature and chemical composition of runoff, impacting aquatic ecosystems. Continued nonplanned urban sprawl and climate change may cause a cascade of detrimental effects on hydrological processes, with far-reaching implications for water resources, ecosystems, and human societies [35,36]. Mitigating these impacts necessitates an integrated and adaptive approach that addresses both climate change and urban planning.

To date, many studies have explored the adverse effects of impervious surfaces on the rise of destructive floods. Based on the above situation, low impact development (LID) solutions can be used as increasingly valuable and urgent solutions, which suggests that decision makers take flood prevention measures in advance to minimize economic losses and casualties [37–39]. Rainwater harvesting (RWH), which belongs to the family of storage-based LID techniques, can be used in urban stormwater management and decrease the risk of flooding through decreasing the frequency, peak and volume of urban runoff if RWH systems are appropriately designed; additionally, water is collected, especially in arid and semiarid areas [40–42]. Urban Stormwater Runoff can be generated from various impervious areas, including rooftops, walkways, patios, driveways, parking lots, storage areas, and concrete or asphalt. In urban areas, especially in dense areas, most land uses involve building roofs, which could be essential methods for rainwater harvesting (S. [43–45]). Therefore, building roofs can be used as an efficient tool for ensuring sustainable environmental and social welfare and for reducing the degree of flooding and increasing the drainage network capacity; this approach can be used by urban managers and decision makers [46–49].

Several advances have been made in analyzing and modeling the effects of building roofs on runoff generation via Multi Criteria Decision Making (MCDA) and hydrological/hydraulic models. The MCDA method is widely used to evaluate the effects of various RWH techniques on the flooding degree. Since these methods work based on expert judgments, the concept of uncertainty in the method is one of the most important barriers to simulating the role of RWH in determining the flooding degree [50,51,28]. The second method is widely used to evaluate the effect of RWH on flooding degree. These hydrological/hydraulic models need extremely accurate local data, which will be suitable for modeling the physical process of waterlogging in small catchments [52–55].

In recent years, the concept of hydrological connectivity (HC) has emerged for delineating spatial patterns of runoff distribution through landscapes and therefore dependent on runoff generation dynamics, the configuration of runoff-generating patches, the routing of flow through a catchment and disconnection impervious areas [56–59]. This approach is key for designing sustainable land management plans at small to large scales [31,60]. To effectively assess hydrological connectivity, various methods, including field observations, tracing methods, graph theory methods, simple index methods, and model simulations, have been developed over time (G. A. [61]; J. [62]). At small scales, hydrological connectivity can be calculated based on field observations directly or indirectly by using intrinsic characteristics that affect runoff generation, such as the topographic wetness index or drainage density (W. [63]). Field-based works are time consuming and costly; therefore, they are suitable for small-scale areas other than large-scale areas [64,65]. In tracing models, the analysis of acquired results due to the existence of external factors for quantifying tracer conservativeness faces a series of problems [66]. Graph theory methods are more suitable for quantifying connectivity at the scale of erosion plots or ephemeral/slope gullies (J. [67,68]). In contrast, Borselli, Cassi, and Torri [69] proposed an index of hydrological connectivity with the merits of high efficiency, simplicity, and low cost; this index has thus become widely applied to assess potential connections in catchments and form the basis for much subsequent modeling [70–72]. The Borselli index is a structural metric linked to landscape geomorphology, describing the spatial contiguity of landscape units. Meanwhile, the functional aspects (process-based), which are linked to hydrological properties, relate to surface and subsurface flow processes operating in different components of the landscape. In this way, the functional connectivity index, derived from the Borselli index, can become a useful tool for landscape management. However, the characterization of hydrologically-driven transfer processes requires further advancements to enhance the understanding of the diffusiveness resulting from human-induced land use activities. Functional connectivity can be used as an effective tool to simulate the role of human interventions in a watershed system [57,73,74]; for example, in RRWH; however, the scientific literature has not yet paid attention to this topic extensively. Therefore, this study proposed a new approach in which the Soil Conservation Service Curve Number (SCS-CN) empirical method was combined with the Borselli index to obtain functional hydrological connectivity. The proposed approach was applied to the city of Hamadan, which is located in Iran, to evaluate runoff variation. The novelty of this study is the proposal of an integrated method applied for the first time in an urban area to evaluate the role of the RWH from rooftops (RRWH) in determining hydrological connectivity (HC). We hypothesize that this study can quantify functional connectivity by combining the SCS-CN method and improve the accuracy of identifying the spatial pattern of functional connectivity in the state of RRWH.

2. Materials and methods

2.1. Study area characteristics

Hamadan city is a historical and cultural city in Iran and was selected for this study (Fig. 1). The case study area is 45 km^2, which is one of the most relevant metropolitan areas in western Iran. Hamadan city is characterized by an annual average temperature of 10 °C and an annual precipitation of 340 mm [75,41]. Rainfall shows high seasonal variability, so most of the events occur from October to January. Due to the existence of agricultural land in the western and eastern parts of the case study area, the main expansion of the city was limited to the northern and southern parts. This issue has caused a great proportion of the population of the city (i.e., >0.55 million people) to be concentrated in the northern to southern regions. In the period from 1998 to 2011, the

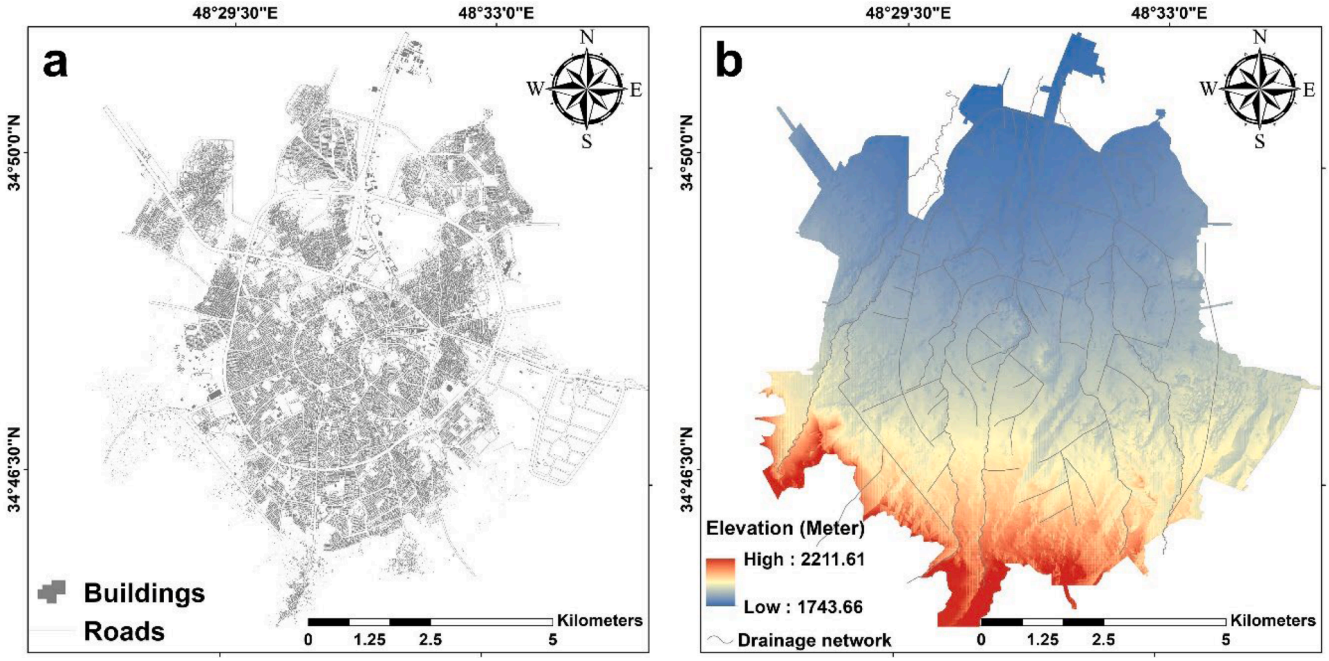

Fig. 1. Location of the case study area: a Building and road map. b Elevation map with drainage network.

territory of built-up areas grew by 29 km^2, and this area is expected to reach 67 km^2, causing the loss of efficiency in the current drainage network to transfer and discharge surface runoff, the latter of which is the most susceptible to flooding (Roumyani, Salehi Mishani, Vosoughi Rod, Ghaderi, and Amraie [76].

2.2. Index of hydrological connectivity (HC)

The index of hydrological connectivity (HC) in this study is based on the index proposed by Borselli et al. [69]. The index indicates the runoff connectivity between hillslopes and a specific depositional point from a geomorphic approach ([77]; M [78]; K. [79,80]). The Borselli connectivity index is a fractional equation (Eq. (1)). The numerator of the HC is related to the upslope component (D_{up}), which represents the potential for downward routing of overland flow occurring upslope and is calculated based on the upslope contributing area (A) (m^2), and the runoff potentials controlled by $\bar{w}$ and $\bar{s}$ are the average weighting factor and slope gradient (m m^{-1}), respectively, of the upslope contributing area. The denominator of the HC (D_{dn}) shows the probability of the runoff-flow path length occurring until it arrives at a defined sink along the flow path, where d_i is the length of pixel i downslope (m) and w_i and s_i are the surface roughness and slope gradient of pixel i, *respectively*.

$$IC = log_{10}\left(\frac{D_{up}}{D_{dn}}\right) = log_{10}\left(\frac{\overline{ws}\sqrt{A}}{\sum_i \frac{d_i}{w_i s_i}}\right) \quad (1)$$

$[-\infty, +\infty]$The lower values of the index ($-\infty$) indicate that the considered element in the analyzed case study functions as a disconnection and generates a lower amount of runoff. The maximum values reached $+\infty$. In this paper, to calculate the whole case study runoff connectivity, the lowest downstream point along the drainage network was considered the sink target.

2.3. Modifications on the HC

In Borselli et al. [69], the variable w_i represents the surface impedance to runoff and sediment fluxes, which is the most important and sensitivity variable, play a main role in HC simulation and quantifying the role of human interventions in a watershed system. Originally, in the calculation of the Borselli et al. [69] index, the values of w_i corresponded to the cover management factor/crop factor, i.e., the C factor of the USLE-RUSLE models [81,82]. Since the C factor refers only to cover and management related to erosion, it has two main disadvantages: (1) it overestimates hydrological connectivity in bare land areas, and (2) this variable represents only the characteristics of cover and does not consider the role of surface roughness [83–85]. In this regard, researchers are trying to develop better options for weighting factors. For example, Nazaripouya et al. [85], based on Cowan's original approach, used a modified Manning's roughness (n) model instead of the C factor of the USLE-RUSLE model. Manning's roughness (n) represents the resistance to flow, with values varying according to the different surface characteristics affecting roughness. In the central Pyrenees, Llena et al. [84] considered both the C factor and topographic variations to better understand the evolution of sediment connectivity associated with different land use and topographic changes. In the other studies, the researchers used the modified version of the Borselli index to better characterize HCs (Table 1).

2.4. Modified version of the hydrological connectivity index

A new approach involving the integration of a rainfall-runoff model and the HC index was proposed for studying spatial and temporal dynamics in the form of functional connectivity. According to several authors ([86,87] and [88]), the SCS-CN model (Eq. (2)) can be used as a w_i factor, as shown in Eq. (1). The method created by the Soil Conservation Act of 1935 is the most widely used method for estimating runoff ([89]; S. K. [90,91]).

$$Q = \frac{(P - 0.2S)^2}{(P + 0.8S)} \qquad if\ P \geq 0.2S \quad (2)$$

$$S = \frac{25400}{CN} - 254 \quad (3)$$

where P is the rainfall (mm), Q is the corresponding runoff (mm), and CN is the curve number, which is a function of land use type, soil hydrological group and soil antecedent moisture condition (AMC) and is used to represent the hydrological behavior of the catchment (USDA SCS

Table 1
Modified version of the Borselli et al. [69] index.

Descriptor	Equation	Reference
The revised Borselli index connectivity (2008) to study spatial and temporal of connectivity at (large) catchment scale	$IC_{revise} = log_{10}\left(\frac{R_t RTC_t K_p S\sqrt{A_k}}{\sum_i \frac{d_i}{AWC_i s_i}}\right)$	(Manuel [45])
	$IC_{revise} = log_{10}\left(\frac{R_t C_t S\sqrt{A_k}}{\sum_i \frac{d_i}{Rt_i C_i s_i}}\right)$	[15]
	$IC_{revise} = log_{10}\left(\frac{\sum iR_i LS_i C_{ti} S_{pixel}}{\left(\sum_i \frac{n_j . d_j}{s_i}\right)_k}\right)$	[20]
The IC was calculated with reference to both targets, i.e., the main channel ($IC_{channel}$) and the basin outlet (IC_{outlet})	$IC_{revise} = \log_{10}\left(\frac{\overline{WS}\sqrt{A_k}}{\sum_i \frac{d_i}{w_i s_i}}\right)$	Mishra et al., [79]
The revised Borselli index connectivity (2008) for lowland areas	$IC_{revise} = \log_{10}\left(\frac{\overline{W}\,\overline{IDPR}\overline{S}\sqrt{A_k}}{\sum_i \frac{d_i}{w_i s_i}}\right)$	Gay et al. [58]

Note: R_t is the normalized rainfall erosivity factor for the period t, RT is the residual topography factor, Ct is the vegetation and crop management factor for the period t, KP is the soil permeability factor, S is the slope gradient, A is upslope contributing area, LS_i is the slope length and steepness factor, IDPR is the index of development and persistence of the drainage network.

[92]). Three types of AMC, namely, the lower limit of moisture (AMCI), average soil moisture content (AMCII) and upper limit of soil moisture (AMCIII), are considered to calculate the CN value (Table 2). The CN values for the AMCII state are derived from the SCS-CN manual, and for the other two antecedent soil moistures, the following equations are used to calculate the CN variable:

$$CNI = \frac{4.2CNII}{(10 - 0.058CNII)} \tag{4}$$

$$CNIII = \frac{23CNII}{(10 + 0.13CNII)} \tag{5}$$

Generally, three types of antecedent soil moisture are defined as dry (lower limit of moisture), moderate (average soil moisture content) and humid (upper limit of soil moisture); these three types of moisture are represented as AMCI, AMCII, and AMCIII, respectively [93,94]. In the AMCII, the CN values are calculated from the SCS-CN manual.

The SCS-CN method has been widely used across different regions, land uses, and climatic conditions. However, when applied to urban environments, it may underestimate runoff volumes, which are crucial for effective flood risk management and stormwater infrastructure planning. In urban areas, connected areas cause changes in the CN value, which refers to how the runoff generated from impervious areas drains to drainage networks [95,45]. If the generated runoff from any impervious land use drains into the next impervious area and then into the drainage network or if the generated runoff directly drains into the drainage network, then the considered impervious land use must be considered a connected area, and its related CN values must be modified to new CN values [95,41]. Distinguishing between connected areas requires some study of surface and subsurface runoff, flow paths, and discharge structures and their connections, which is a complex challenge [95,41]. In the present study, the modified CNs according to connected areas were derived from the studies of Sepehri et al. [41] and Malekinezhad, Sepehri, et al. [45].

Table 2
CN values of the land use types in the study area [41].

Land use	CN
Park and Garden	61
Cultural and administrative buildings, sports, military	69
Health and educational buildings, office, hotel, residential, religious	85
Parking, commercial, industry and workshop	92
Coach terminal, bus terminal, roads, streets, pavement	95

After the calculation of the SCS-CN model, the wi factor was replaced with the w_i factor in the Borselli et al. [69] index, after which the functional connectivity was extracted as follows:

$$IC = log_{10}\left(\frac{\overline{Q}\sqrt{A}}{\sum_i \frac{d_i}{Q_i s_i}}\right) \tag{6}$$

Eq. (6) is used to evaluate the spatial distribution of HCs in the absence of RRWH. To consider the RRWH, the capacity of the RRWH (Eq. (7)) must be subtracted from the Q parameter; consequently, Eq. (6) will be transferred to Eq. (8).

$$RRWH = \frac{Q * TRA * ECA * (1 - CL - FF)}{1000} \tag{7}$$

$$IC = \left(\frac{(\overline{Q} - RRWH)\sqrt{A}}{\sum_i \frac{d_i}{(Q_i - RRWH_i)s_i}}\right) \tag{8}$$

where TRA is the total rooftop area (m^2), ECA is the effective collection area, CL is the collection loss and FF refers to the first flush.

2.4. Data acquisition and preprocessing

Most of the variables used in the HC equation, including A, d_i and s_i, are calculated from a digital elevation model (DEM). Additionally, the slope parameter has a direct relationship with the CN value according to the SCS-CN method. Therefore, the accuracy of the HCs is a function of the DEM. Before preparing DEMs in urban areas, which reveal the complexity of surface features, the degree of urbanization is the key factor that enhances the sophistication of environmental studies. The impervious land uses, such as buildings, roads, and pavements, in urban areas, which are known as hared features, are called fine constrained features (FCFs) [96]. These features certainly disturb surface features and runoff propagation. Therefore, FCF_s must be considered in the preparation of DEMs. In the present study, the algorithm of the constrained Delaunay triangle irregular network (CD-TIN) associated with a scale of 1/2000 elevation maps were used to model the complexity of urban surfaces and their details (More descriptions can be found in [96] and [75]). In the elevation maps used, the digital elevations were taken from the roofs of buildings and floors of streets. Additionally, in this algorithm, the borders of the FCFs were entered as Constrain features (Table 3). Fig. 2 shows a schematic of the CD-TIN algorithm on one of the buildings in the case study. To calculate the CN value via the SCS-CN method, the land use data of the case study with a resolution of 2 m were obtained from the General Administration of Hamadan Province Municipality. According to Malekinezhad, Sepehri, et a-l. [45], in a rainfall event with a 50-year return period (50 mm), the whole of the case study involved runoff production; therefore, in the present study, only the

Table 3
FCFs and their data types in the CD_TIN algorithm [96].

Constrain Features	Type	Data Organization
Road cambers, Street curbs, Walls, etc.	Constrained polyline	Shape file Polyline
Buildings, Parks, Playgrounds, etc.	Constrained polyline	Shape file Polygon

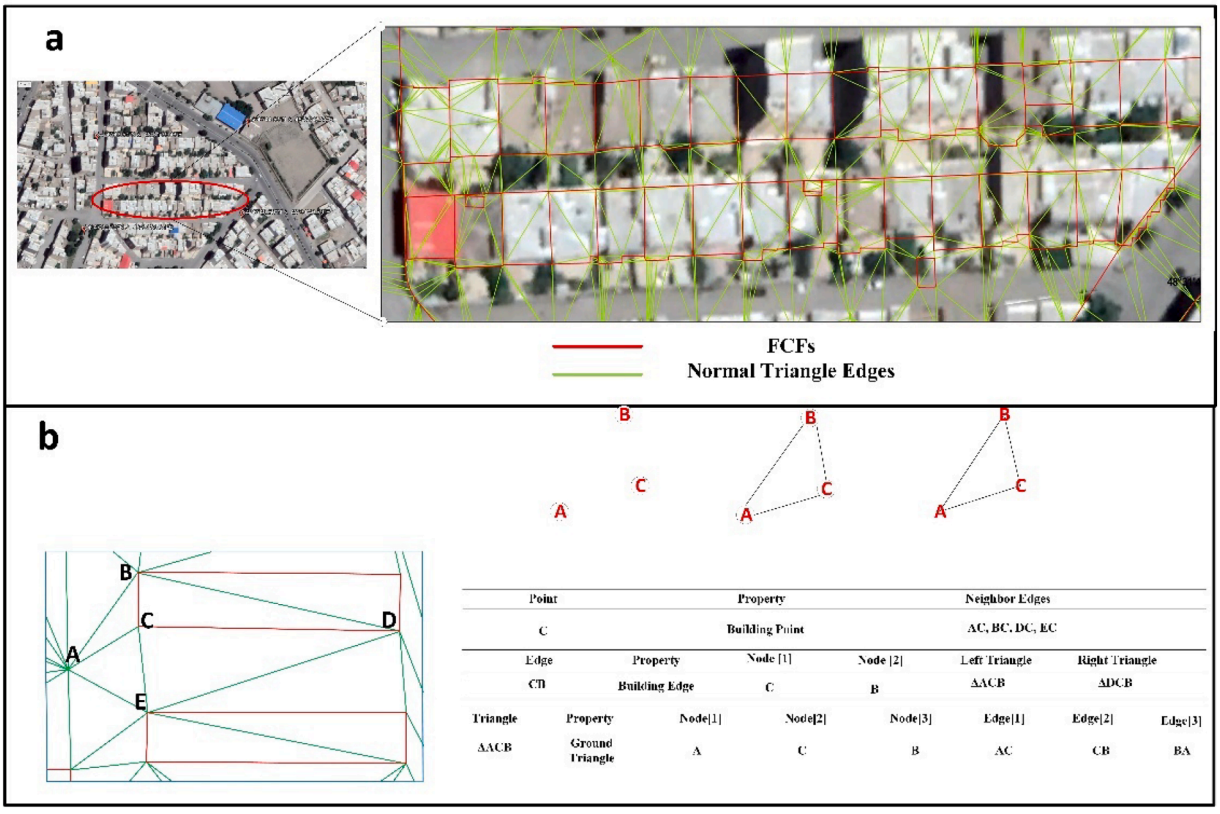

Fig. 2. a Sample schematic of the CD-TIN algorithm in the case study, b The red lines represent constrained features, like buildings and street curbs, while the green lines denote the edges of the normal triangles. [75].

mentioned return period was used for calculating the P value in the SCS-CN method.

3. Results and discussion

Several attempts have been made to assess the effects of LID practices on hydrological connectivity. Hamadan city was chosen as the case study area. Fig. 3 shows the reclassified spatial distribution of hydrological connectivity values using the natural breaks method in ArcGIS 10.7 for the catchment without RRWH practices. The method employs the Jenks algorithm to detect natural breakpoints, where the most significant gaps between data values are found. It then groups the data into classes that have low internal variance and high inter-class differences, ensuring each class contains similar characteristics. The areas of the HC classes, i.e., very low (−2.9, −0.92), low (−0.92, −0.07), moderate (−0.07, 0.63), high (0.63, 1.34) and very high (1.34, 3.38), are 9.2, 19.6, 26.8, 25.5 and 15.7 m^2, respectively. The very low and low classes of HCs were clearly identified in the southern region of the patient cohort. These areas are characterized by lower values of d_i and steep hill slopes. From the southern to the northern parts, there are sudden changes in the slope and elevation properties of the case study, which results in different hydrological behaviors. Therefore, the other classes of hydrological connectivity, i.e., moderate, high and very high connectivity degrees, are located in the middle and northern parts of the case study area. To better describe the HCs in these areas, two locations were selected for evaluation. The *A* location is one of the subareas located in the very high HC. In this location, which is an ancient area, ancient excavations show that these areas have been destroyed due to the occurrence of large floods [97,75]. The B location is the area that, despite having a slope and d_i parameter, has the maximum road density and moderate density of buildings, which leads to a divergence in the flow direction and increase in the CN values and, consequently, in the value of the Q parameter in the HC equation. The C location is called Madani town, and its features are nearly similar to those of the B region; in this region, the density of buildings is high, and nearly 36,000 people live in this region. Additionally, in this region, the values of the slope and d_i parameter are very low [97,75].

The spatial distribution of HCs in the presence of RRWH is shown in Fig. 4. To construct this map, first, the variable RWH in Eq. (7), which is one of the main steps in calculating this HC, was calculated. Since the climate of the case study area is semiarid, the percentage of pitch rooftops is nearly negligible; therefore, the value of the ERA was considered 100 %. All the captured rainwater that is saved in cisterns cannot be consumed. Some of the captured defects will be lost due to the kind of design cistern. According to Sepehri et al. [41], Malekinezhad, Sepehri, et al. [98] and Meshram et al. [39], a well-designed cistern must have a maximum value of 10 %, so in this study, a value of 10 % was considered for the CL value. Then, some of the captured runoff must be used to clean insects, feces, etc. In this paper, a value of 20 % was considered for the FF parameter. The reclassification table of HCs in the absence of RRWH, which is the baseline of this comparison, was subsequently used to reclassify the values of HCs in the presence of RRWH. A comparison of two acquired HCs revealed significant differences in the HC values and the areas of the HC classes; by applying the RRWH, the areas of very high (1.34, 7.78) and high (0.63, 1.34) HCs in the absence of RRWH reached 11.4 and 20.4 m^2, respectively. The areas with remaining HC classes, including moderate (−0.07, 0.63), low (−0.92, −0.07) and very low (−6.7, −0.92) HCs, exhibited increases of 27.9, 28.4 and 11.7 m^2, respectively (Fig. 5). Analysis of the HCs suggested that RRWH have a notable effect on decreasing HCs; one of the main reasons for this decrease is related to the percentage of existing buildings in the case study, in which only residential buildings accounted for 32 % of the total land use (Table. S1 represent the land use types and their covered area). The influence of RRWH on reducing runoff phenomena has been examined in many studies at different spatial scales and resolutions; thus, the results of this study agree with the observations

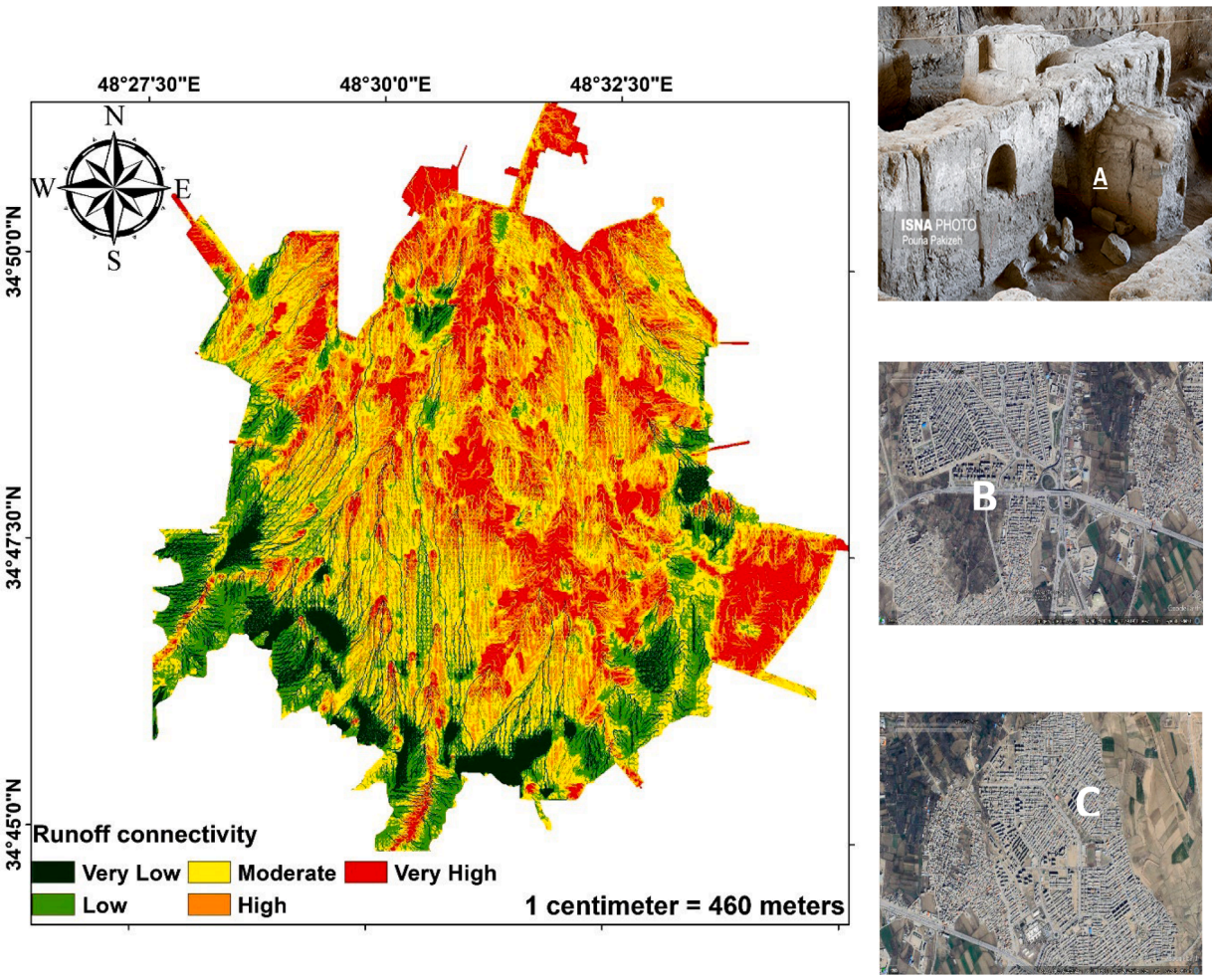

Fig. 3. Spatial distribution of HCs without RRWH.

reported in the available literature. For instance, Sepehri et al. [41] used the HEC—HMS model to measure the effect of RRWH on reducing runoff volume. Malekinezhad, Sepehri, et al. [98] evaluated the role of RRWH as a rooftop disconnection for increasing the capacity of drainage networks and consequently reducing the risk of floods. Nishigaki, Sugihara, Kilasara, and Funakawa [99] concluded that the runoff volume and sediment concentration at sites associated with LID practices are lower than those at other sites with the same rainfall depth.

4. Conclusion

The index of hydrological connectivity can be used as an effective tool for analyzing catchment changes, especially in urban areas where man-made built elements change the hydrological behavior of the catchment. In this study, a revised index of Borselli connectivity was developed using the SCS-CN method, allowing the generation of realistic spatial variability in connectivity and the evaluation of the role of LID practices. The simulation of HCs in the absence of RRWHs showed that the areas with very high and high degrees of HCs were located in the middle and northern parts of the study area, where the density of man-made built areas was greatest. By implementing the RRWH, a significant change occurred in the spatial distribution of HCs calculated in the absence of RRWH, so that by applying the RRWH, the areas of very high and high degrees of HCs in the absence of RRWH reached 11.4 and 20.4 m^2, respectively. In addition to reducing flood risk, incorporating roof rainwater harvesting (RRWH) into urban planning provides several key benefits, including enhanced water management and greater sustainability. Promoting RRWH through regulations, incentives, and public awareness can help lower urban water demand, alleviate pressure on infrastructure, and strengthen climate resilience. Furthermore, these policies can promote more equitable access to water, particularly in regions facing water scarcity.

CRediT authorship contribution statement

Quang-Oai Lu: Writing – review & editing, Writing – original draft, Validation, Formal analysis, Conceptualization. **Reza Bahramloo:** Writing – original draft, Visualization, Software, Methodology, Formal analysis. **Jesús Rodrigo-Comino:** Writing – review & editing, Writing – original draft, Visualization. **Jun Wang:** Writing – review & editing, Writing – original draft, Visualization, Methodology. **Ali Talebi:** Writing – original draft, Formal analysis, Data curation. **Quynh Thi Phuong Tran:** Writing – review & editing, Validation, Supervision, Formal analysis, Conceptualization. **Afshin Ghahramani:** Writing – original draft, Visualization, Formal analysis, Conceptualization. **Mehdi Sepehri:** Writing – original draft, Visualization, Methodology, Data curation, Conceptualization.

Declaration of competing interest

The authors declare that they have no known competing financial interests or personal relationships that could have appeared to influence the work reported in this paper.

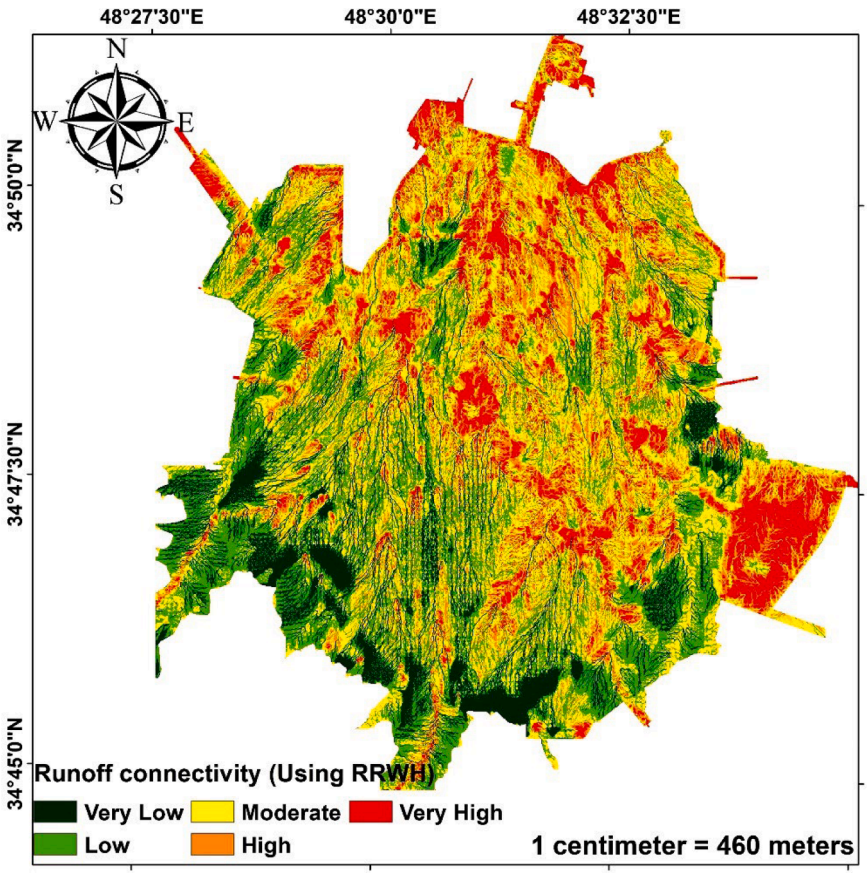

Fig. 4. Spatial distribution of HCs in the presence of RRWH.

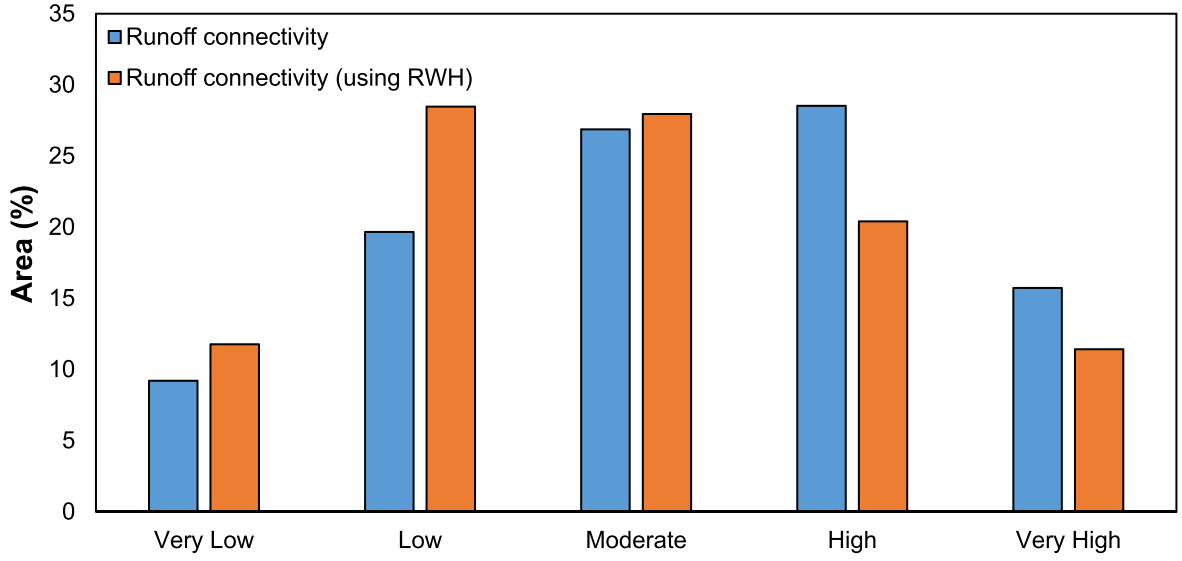

Fig. 5. Area percentages of HC classes in the absence/presence of RWH.

Supplementary materials

Supplementary material associated with this article can be found, in the online version, at doi:10.1016/j.rineng.2025.104022.

Data availability

Data will be made available on request.

References

[1] R. Bahramloo, J. Wang, M. Sepehri, A. Faghfouri, B. Ghermezcheshmeh, A. Atapourfard, E. Bazrafshan, Novel MCDA methods for flood hazard mapping: a case study in Hamadan, Iran, Stochast. Environ. Res. Risk Assessm. (2024) 1–19.

[2] G. Dharmarathne, A. Waduge, M. Bogahawaththa, U. Rathnayake, D. Meddage, Adapting cities to the surge: a comprehensive review of climate-induced urban flooding, Result. Eng. (2024) 102123.

[3] N. Mohammed, P. Palaniandy, F. Shaik, B. Deepanraj, H. Mewada, Statistical analysis by using soft computing methods for seawater biodegradability using ZnO photocatalyst, Environ. Res. 227 (2023) 115696.
[4] M.W. Saleem, M. Rashid, S. Haider, M. Khalid, A. Elfeki, Simulation of urban flooding using 3D computational fluid dynamics with turbulence model, Result. Eng. (2024) 103609.
[5] U. Nkwunonwo, M. Whitworth, B. Baily, A review of the current status of flood modelling for urban flood risk management in the developing countries, Scientif. Afr. 7 (2020) e00269.
[6] A. Pallathadka, J. Sauer, H. Chang, N.B. Grimm, Urban flood risk and green infrastructure: who is exposed to risk and who benefits from investment? A case study of three US Cities, Landsc. Urban Plan. 223 (2022) 104417.
[7] M.V.C. Rodrigues, D.V. Guimarães, R.B. Galvao, E. Patrick, F. Fernandes, Urban watershed management prioritization using the rapid impact assessment matrix (RIAM-UWMAP), GIS and field survey, Environ. Impact. Assess. Rev. 94 (2022) 106759.
[8] R. Ahmed, S.T. Ahmad, G.F. Wani, P. Ahmed, A.A. Mir, A. Singh, Analysis of landuse and landcover changes in Kashmir valley, India—a review, GeoJournal 87 (5) (2022) 4391–4403.
[9] S. Bell, S. Alves, E.S. de Oliveira, A. Zuin, Migration and land use change in Europe: a review, Living Rev. Landsc. Res. 4 (2) (2010) 1–49.
[10] N. Mohammed, P. Palaniandy, F. Shaik, Pollutants removal from saline water by solar photocatalysis: a review of experimental and theoretical approaches, Int. J. Environ. Anal. Chem. 103 (16) (2023) 4155–4175.
[11] H.I. Rizvi, R.M. Munir, T. Iqbal, A. Younas, S. Afsheen, M.T. Qureshi, K. Riaz, Novel existence of Mn and Cu in WO3 nanostructures for promising photocatalytic activity against MB dye and Levofloxacin antibiotic, J. Alloy. Compd. 993 (2024) 174549.
[12] N.N. Devi, B. Sridharan, S.N. Kuiry, Impact of urban sprawl on future flooding in Chennai city, India, J. Hydrol. 574 (2019) 486–496.
[13] D. Hou, F. Meng, A.V. Prishchepov, How is urbanization shaping agricultural land-use? Unraveling the nexus between farmland abandonment and urbanization in China, Landsc. Urban Plan. 214 (2021) 104170.
[14] J. Hubbart, Urban Ecosystems: alterations to Peakflow, Microclimate and the Natural Environment, Nature Precedings (2009) 1. -1.
[15] H. Storch, N.K. Downes, A scenario-based approach to assess Ho Chi Minh City's urban development strategies against the impact of climate change, Cities 28 (6) (2011) 517–526.
[16] B.T. Hassan, M. Yassine, D. Amin, Comparison of urbanization, climate change, and drainage design impacts on urban flashfloods in an arid region: case study, New Cairo, Egypt, Water (Basel) 14 (15) (2022) 2430.
[17] T. Iqbal, M. Afzal, B.A. Al-Asbahi, S. Afsheen, I. Maryam, A. Mushtaq, A. Ashraf, Enhancing apple shelf life: a comparative analysis of photocatalytic activity in pure and manganese-doped ZnO nanoparticles, Mater. Sci. Semicond. Process. 173 (2024) 108152.
[18] G. Shatkin, Futures of crisis, futures of urban political theory: flooding in Asian coastal megacities, Int. J. Urban Reg. Res. 43 (2) (2019) 207–226.
[19] Z. Tang, P. Wang, Y. Li, Y. Sheng, B. Wang, N. Popovych, T. Hu, Contributions of climate change and urbanization to urban flood hazard changes in China's 293 major cities since 1980, J. Environ. Manage. 353 (2024) 120113.
[20] S. Du, P. Shi, A. Van Rompaey, J. Wen, Quantifying the impact of impervious surface location on flood peak discharge in urban areas, Nat. Hazard. 76 (2015) 1457–1471.
[21] P. Gong, X. Li, J. Wang, Y. Bai, B. Chen, T. Hu, W. Zhang, Annual maps of global artificial impervious area (GAIA) between 1985 and 2018, Remote Sens. Environ. 236 (2020) 111510.
[22] X. Zhang, L. Liu, T. Zhao, Y. Gao, X. Chen, J. Mi, GISD30: global 30 m impervious-surface dynamic dataset from 1985 to 2020 using time-series Landsat imagery on the Google Earth Engine platform, Earth Syst. Sci. Data 14 (4) (2022) 1831–1856.
[23] E. Bozzolan, E.A. Holcombe, F. Pianosi, I. Marchesini, M. Alvioli, T. Wagener, A mechanistic approach to include climate change and unplanned urban sprawl in landslide susceptibility maps, Sci. Tot. Environ. 858 (2023) 159412.
[24] M. Faheem, T. Iqbal, S. Afsheen, A. Basit, R.M. Munir, M.I. Khan, H.I. Rizvi, A maghemite (γ-Fe2O3) incorporated activated carbon photocatalytic nanocomposite fabricated via Co-precipitation utilized against degradation of methyl orange, Opt. Mater. 157 (2024) 116131.
[25] X. Ju, W. Li, J. Li, L. He, J. Mao, L. Han, Future climate change and urban growth together affect surface runoff in a large-scale urban agglomeration, Sustain. Citi. Soc. 99 (2023) 104970.
[26] W. Yang, Z. Zhao, L. Pan, R. Li, S. Wu, P. Hua, J. Zhang, Integrated risk analysis for urban flooding under changing climates, Result. Eng. 24 (2024) 103243.
[27] G. Chataut, B. Bhatta, D. Joshi, K. Subedi, K. Kafle, Greenhouse gases emission from agricultural soil: a review, J. Agricult. Food Res. (2023) 100533.
[28] M. Nayeemuddin, P. Palaniandya, F. Shaik, H. Mewada, Experimental and computational analysis for optimization of seawater biodegradability using photo catalysis, IIUM Eng. J. 24 (2) (2023) 11–33.
[29] A. D'Agata, D. Ponza, F.A. Stroiu, I. Vardopoulos, K. Rontos, F. Escrivà, S. S. Nickyain, Toward sustainable development trajectories? Estimating urban footprints from high-resolution copernicus layers in Athens, Greece, Land (Basel) 12 (8) (2023) 1490.
[30] C. Gramaglia, M. Rio, C. Salles, M.-G. Tournoud, Reducing the imperviousness of urban soils to enhance the quality of surface water: obstacles and levers to implementing ecological runoff management in the south of France, J. Hydrol. 636 (2024) 131168.
[31] N. Mohammed, P. Palaniandy, F. Shaik, Optimization of solar photocatalytic biodegradability of seawater using statistical modelling, J. India. Chem. Soc. 98 (12) (2021) 100240.
[32] A. Pérez-Morales, A. Romero-Díaz, E. Illán-Fernandez, Rainfall, anthropogenic soil sealing, and floods. An example from southeastern Spain. Precipitation, Elsevier, 2021, pp. 499–520.
[33] J. Senciales-González, J. Rodrigo-Comino, P. Smith, Surveying topographical changes and climate variations to detect the urban heat island in the city of Málaga (Spain), Cuadernos de Investigación Geográfica 46 (2) (2020) 521–543.
[34] E.T. Steinke, V.A. Steinke, R.R. da Franca, Geographic analysis of flooding in the urban area of the Federal District, Brazil. Urban Flooding in Brazil, Springer, 2023, pp. 275–295.
[35] M. Marselina, S.A. Nurhayati, S.L. Pandia, Flood analysis and estimating economic losses in an affected area (case study: cikapundung watershed), Air Soil Water Res. 15 (2022) 11786221221131277.
[36] A. Younas, R.M. Munir, H.I. Rizvi, T. Iqbal, S. Afsheen, K. Riaz, L.S. Wong, Novel S–N/WO3: optimization of photocatalytic performance of WO3 by simultaneous existence of S and N in WO3 against MB dye, J. Chem. Phys. 160 (24) (2024).
[37] M.O. Arjenaki, H.R.Z. Sanayei, H. Heidarzadeh, N.A. Mahabadi, Modeling and investigating the effect of the LID methods on collection network of urban runoff using the SWMM model (case study: shahrekord City), Model. Earth Syst. Environ. 7 (1) (2021) 1–16.
[38] M.A. Jemberie, A.M. Melesse, Urban flood management through urban land use optimization using LID techniques, city of Addis Ababa, Ethiopia, Water (Basel) 13 (13) (2021) 1721.
[39] S.G. Meshram, A.R. Ilderomi, M. Sepehri, F. Jahanbakhshi, M. Kiani-Harchegani, A. Ghahramani, J. Rodrigo-Comino, Impact of roof rain water harvesting of runoff capture and household consumption, Environ. Sci. Pollut. Res. 28 (2021) 49529–49540.
[40] A. Campisano, D. Butler, S. Ward, M.J. Burns, E. Friedler, K. DeBusk, H. Furumai, Urban rainwater harvesting systems: research, implementation and future perspectives, Water Res. 115 (2017) 195–209.
[41] M. Sepehri, H. Malekinezhad, A.R. Ilderomi, A. Talebi, S.Z. Hosseini, Studying the effect of rain water harvesting from roof surfaces on runoff and household consumption reduction, Sustain. Citi. Soc. 43 (2018) 317–324.
[42] Valdiviezo Gonzales, L.G., García-Ávila, F., Guanoquiza-Suárez, M., Guzmán-Galarza, J., & Cabello-Torres, R. (2023). Rainwater harvesting and storage systems for domestic supply: an overview of research for water scarcity management in rural areas.
[43] S. Ali, Y.-F. Sang, Implementing rainwater harvesting systems as a novel approach for saving water and energy in flat urban areas, Sustain. Citi. Soc. 89 (2023) 104304.
[44] Y.-R. Chiu, K. Aghaloo, B. Mohammadi, Incorporating rainwater harvesting systems in iran's potable water-saving scheme by using a GIS-simulation based decision support system, Water (Basel) 12 (3) (2020) 752.
[45] H. Malekinezhad, M. Sepehri, S.Z. Hosseini, C.A.G. Santos, J. Rodrigo-Comino, S. G. Meshram, Role and concept of rooftop disconnection in terms of runoff volume and flood peak quantity, Int. J. Environ. Res. 15 (2021) 935–946.
[46] F.A. Abdulla, A.W. Al-Shareef, Roof rainwater harvesting systems for household water supply in Jordan, Desalination 243 (1–3) (2009) 195–207.
[47] M.D. Kumar, Roof water harvesting for domestic water security: who gains and who loses? Water Int. 29 (1) (2004) 43–53.
[48] C.M. Monteiro, C.S. Calheiros, C. Pimentel-Rodrigues, A. Silva-Afonso, P.M. Castro, Contributions to the design of rainwater harvesting systems in buildings with green roofs in a Mediterranean climate, Water Sci. Technol. 73 (8) (2016) 1842–1847.
[49] B. Pirouz, S.A. Palermo, M. Turco, Improving the efficiency of green roofs using atmospheric water harvesting systems (an innovative design), Water (Basel) 13 (4) (2021) 546.
[50] M.M. de Brito, A. Almoradie, M. Evers, Spatially-explicit sensitivity and uncertainty analysis in a MCDA-based flood vulnerability model, Int. J. Geograph. Inform. Sci. 33 (9) (2019) 1788–1806.
[51] N. Mohammed, P. Palaniandy, F. Shaik, H. Mewada, D. Balakrishnan, Comparative studies of RSM Box-Behnken and ANN-Anfis fuzzy statistical analysis for seawater biodegradability using TiO2 photocatalyst, Chemosphere 314 (2023) 137665.
[52] P. Bates, M. Horritt, C. Smith, D. Mason, Integrating remote sensing observations of flood hydrology and hydraulic modelling, Hydrol. Process. 11 (14) (1997) 1777–1795.
[53] G. Di Baldassarre, G. Schumann, P.D. Bates, A technique for the calibration of hydraulic models using uncertain satellite observations of flood extent, J. Hydrol. 367 (3–4) (2009) 276–282.
[54] D. Mehta, J. Dhabuwala, S.M. Yadav, V. Kumar, H.M. Azamathulla, Improving flood forecasting in Narmada river basin using hierarchical clustering and hydrological modelling, Result. Eng. 20 (2023) 101571.
[55] G. Schumann, P.D. Bates, M.S. Horritt, P. Matgen, F. Pappenberger, Progress in integration of remote sensing–derived flood extent and stage data and hydraulic models, Rev. Geophys. 47 (4) (2009).
[56] L.J. Bracken, J. Croke, The concept of hydrological connectivity and its contribution to understanding runoff-dominated geomorphic systems, Hydrolog. Process.: Int. J. 21 (13) (2007) 1749–1763.
[57] L.J. Bracken, J. Wainwright, G. Ali, D. Tetzlaff, M. Smith, S. Reaney, A. Roy, Concepts of hydrological connectivity: research approaches, pathways and future agendas, Earth-Sci. Rev. 119 (2013) 17–34.
[58] A. Gay, O. Cerdan, V. Mardhel, M. Desmet, Application of an index of sediment connectivity in a lowland area, J. Soil. Sedim. 16 (2016) 280–293.
[59] I. Lexartza-Artza, J. Wainwright, Hydrological connectivity: linking concepts with practical implications, Catena 79 (2) (2009) 146–152.

[60] Y. Yu, J. Feng, H. Liu, C. Wu, J. Zhang, Z. Wang, J. Rodrigo-Comino, Linking hydrological connectivity to sustainable watershed management in the Loess Plateau of China, Curr. Opin. Environ. Sci. Health (2023) 100493.
[61] G.A. Ali, A.G. Roy, M.-C. Turmel, F. Courchesne, Source-to-stream connectivity assessment through end-member mixing analysis, J. Hydrol. 392 (3–4) (2010) 119–135.
[62] J. Yang, X. Chu, Effects of DEM resolution on surface depression properties and hydrologic connectivity, J. Hydrolog. Eng. 18 (9) (2013) 1157–1169.
[63] W. Liu, C. Shi, Y. Ma, Y. Wang, Evaluating sediment connectivity and its effects on sediment reduction in a catchment on the Loess Plateau, China, Geoderma 408 (2022) 115566.
[64] M. Delmas, O. Cerdan, J.-M. Mouchel, M. Garcin, A method for developing a large-scale sediment yield index for European river basins, J. Soil. Sedim. 9 (2009) 613–626.
[65] N. Mohammed, P. Palaniandy, F. Shaik, H. Mewada, Statistical modelling of solar photocatalytic biodegradability of seawater using combined photocatalysts, J. Instit. Eng. (India): Ser. E 104 (2) (2023) 251–267.
[66] S. Najafi, D. Dragovich, T. Heckmann, S.H. Sadeghi, Sediment connectivity concepts and approaches, Catena 196 (2021) 104880.
[67] J. Liu, B.A. Engel, L. Dai, Y. Wang, Y. Wu, G. Yan, M. Zhang, Capturing hydrological connectivity structure of wetlands with indices based on graph theory: a case study in Yellow River Delta, J. Clean. Prod. 239 (2019) 118059.
[68] G. Zuecco, M. Rinderer, D. Penna, M. Borga, H. Van Meerveld, Quantification of subsurface hydrologic connectivity in four headwater catchments using graph theory, Sci. Tot. Environ. 646 (2019) 1265–1280.
[69] L. Borselli, P. Cassi, D. Torri, Prolegomena to sediment and flow connectivity in the landscape: a GIS and field numerical assessment, Catena 75 (3) (2008) 268–277.
[70] M. López-Vicente, S. Álvarez, Influence of DEM resolution on modelling hydrological connectivity in a complex agricultural catchment with woody crops, Earth Surface Process. Landform. 43 (7) (2018) 1403–1415.
[71] J.F. Martínez-Murillo, M. López-Vicente, Effect of salvage logging and check dams on simulated hydrological connectivity in a burned area, Land Degrad. Develop. 29 (3) (2018) 701–712.
[72] A.J. Ortíz-Rodríguez, C. Muñoz-Robles, L. Borselli, Changes in connectivity and hydrological efficiency following wildland fires in Sierra Madre Oriental, Mexico, Sci. Tot. Environ. 655 (2019) 112–128.
[73] M. Rinderer, G. Ali, L.G. Larsen, Assessing structural, functional and effective hydrologic connectivity with brain neuroscience methods: state-of-the-art and research directions, Earth-Sci. Rev. 178 (2018) 29–47.
[74] P.M. Saco, J.F. Rodríguez, M. Moreno-de las Heras, S. Keesstra, S. Azadi, S. Sandi, M.J. Rossi, Using hydrological connectivity to detect transitions and degradation thresholds: applications to dryland systems, Catena 186 (2020) 104354.
[75] M. Sepehri, H. Malekinezhad, S.Z. Hosseini, A.R. Ildoromi, Assessment of flood hazard mapping in urban areas using entropy weighting method: a case study in Hamadan city, Iran, Acta Geophysica 67 (5) (2019) 1435–1449.
[76] A. Roumyani, H. Salehi Mishani, L. Vosoughi Rod, B. Ghaderi, S. Amraie, Application of RS-GIS models in urban expansion optimization with emphasis on environmental protection (Case study: Hamedan City), J. Geogr. Region. Develop. 14 (2) (2017) 51–66.
[77] C. Fernández, J.M. Fernández-Alonso, J.A. Vega, Exploring the effect of hydrological connectivity and soil burn severity on sediment yield after wildfire and mulching, Land Degrad. Develop. 31 (13) (2020) 1611–1621.
[78] M. López-Vicente, J. González-Romero, M. Lucas-Borja, Forest fire effects on sediment connectivity in headwater sub-catchments: evaluation of indices performance, Sci. Tot. Environ. 732 (2020) 139206.
[79] K. Mishra, R. Sinha, V. Jain, S. Nepal, K. Uddin, Towards the assessment of sediment connectivity in a large Himalayan river basin, Sci. Tot. Environ. 661 (2019) 251–265.
[80] M. Sepehri, A. Ghahramani, M. Kiani-Harchegani, A.R. Ildoromi, A. Talebi, J. Rodrigo-Comino, Assessment of drainage network analysis methods to rank sediment yield hotspots, Hydrolog. Sci. J. 66 (5) (2021) 904–918.
[81] K.G. Renard, Predicting Soil Erosion By water: a Guide to Conservation Planning With the Revised Universal Soil Loss Equation (RUSLE), United States Government Printing, 1997.
[82] W.H. Wischmeier, D.D. Smith, Predicting Rainfall Erosion Losses: a Guide to Conservation Planning, Department of Agriculture, Science and Education Administration, 1978.
[83] O. Djoukbala, M. Hasbaia, O. Benselama, M. Mazour, Comparison of the erosion prediction models from USLE, MUSLE and RUSLE in a Mediterranean watershed, case of Wadi Gazouana (NW of Algeria), Model. Earth Syst. Environ. 5 (2) (2019) 725–743.
[84] M. Llena, D. Vericat, M. Cavalli, S. Crema, M. Smith, The effects of land use and topographic changes on sediment connectivity in mountain catchments, Sci. Tot. Environ. 660 (2019) 899–912.
[85] H. Nazaripouya, M. Sepehri, A. Atapourfard, B. Ghermezcheshme, C.A.G. Santos, M. Khoshbakht, Q.B. Pham, Evaluating sediment yield response to watershed management practices (WMP) by employing the concept of sediment connectivity, Sustainability 15 (3) (2023) 2346.
[86] C. Chartin, O. Evrard, J.P. Laceby, Y. Onda, C. Ottlé, I. Lefèvre, O. Cerdan, The impact of typhoons on sediment connectivity: lessons learnt from contaminated coastal catchments of the Fukushima Prefecture (Japan), Earth Surface Process. Landform. 42 (2) (2017) 306–317.
[87] M. López-Vicente, N. Ben-Salem, Computing structural and functional flow and sediment connectivity with a new aggregated index: a case study in a large Mediterranean catchment, Sci. Tot. Environ. 651 (2019) 179–191.
[88] B. De Walque, A. Degré, A. Maugnard, C.L. Bielders, Artificial surfaces characteristics and sediment connectivity explain muddy flood hazard in Wallonia, Catena 158 (2017) 89–101.
[89] W. Boughton, A review of the USDA SCS curve number method, Soil Res. 27 (3) (1989) 511–523.
[90] S.K. Mishra, V.P. Singh, Long-term hydrological simulation based on the Soil Conservation Service curve number, Hydrol. Process. 18 (7) (2004) 1291–1313.
[91] K.X. Soulis, Estimation of SCS Curve Number variation following forest fires, Hydrolog. Sci. J. 63 (9) (2018) 1332–1346.
[92] SCS USDA. National Engineering Handbook, Supplement a, Section 4, US Department of Agriculture, Washington DC, 1985.
[93] K.X. Soulis, Soil Conservation Service Curve Number (SCS-CN) Method: Current applications, Remaining challenges, and Future Perspectives, 13, MDPI, 2021, p. 192.
[94] S. Verma, P. Singh, S.K. Mishra, V. Singh, V. Singh, A. Singh, Activation soil moisture accounting (ASMA) for runoff estimation using soil conservation service curve number (SCS-CN) method, J. Hydrol. 589 (2020) 125114.
[95] J. Hwang, D.S. Rhee, Y. Seo, Implication of directly connected impervious areas to the mitigation of peak flows in urban catchments, Water (Basel) 9 (9) (2017) 696.
[96] Z. Li, L. Wu, W. Zhu, M. Hou, Y. Yang, J. Zheng, A new method for urban storm flood inundation simulation with fine CD-TIN surface, Water (Basel) 6 (5) (2014) 1151–1171.
[97] H. Malekinezhad, M. Sepehri, Q.B. Pham, S.Z. Hosseini, S.G. Meshram, M. Vojtek, J. Vojteková, Application of entropy weighting method for urban flood hazard mapping, Acta Geophys. 69 (3) (2021) 841–854.
[98] H. Malekinezhad, M. Sepehri, S.Z. Hosseini, C.A.G. Santos, J. Rodrigo-Comino, S. G. Meshram, Role and Concept of Rooftop Disconnection in Terms of Runoff Volume and Flood Peak Quantity, Int. J. Environ. Res. 15 (6) (2021) 935–946.
[99] T. Nishigaki, S. Sugihara, M. Kilasara, S. Funakawa, Surface runoff generation and soil loss under different soil and rainfall properties in the Uluguru Mountains, Tanzania, Land Degrad. Develop. 28 (1) (2017) 283–293.